# THE INFLUENCE OF SUBPIXEL MEASUREMENT ON DIGITAL CAMERA CALIBRATION

Mauricio Galo, Antonio M. G. Tommaselli, Júlio K. Hasegawa

UNESP - Univ Estadual Paulista
Faculty of Sciences and Technology (FCT), Department of Cartography
Postgraduate Program in Cartographic Sciences (PPGCC)
Rua Roberto Simonsen, 305, Centro Educacional 19060-900, Presidente Prudente, SP, Brazil
{galo, tomaseli, hasegawa}@fct.unesp.br

**Résumé**

Le but de cette étude est d'évaluer l'influence de la mesure de points dans les images avec une précision subpixellaire, et sa contribution à l'étalonnage des caméras numériques. De plus, l'effet des mesures subpixellaires sur la détermination des coordonnées 3D dans l'espace objet est évalué à partir de points de contrôle. Dans ce but, un algorithme semi-automatique a été implémenté pour la détermination subpixellaire de points d'intérêt, basé sur un opérateur de Förstner. Des expériences ont été réalisées sur un bloc d'images acquises avec une caméra multispectrale DuncanTech MS3100-CIR. L'influence des mesures subpixellaires dans un ajustement par moindres carrés a été évaluée en comparant l'écart-type estimé des paramètres dans deux cas : avec une mesure manuelle (précision pixellaire) et avec une estimation subpixellaire. De plus, l'influence des mesures subpixellaires sur la reconstruction 3D a été analysée. A partir des résultats obtenus, i.e. la réduction de l'écart-type sur les paramètres d'orientation interne et de l'erreur relative de la reconstruction 3D, il est démontré que les mesures de précision subpixellaire sont pertinentes pour certains travaux photogrammétriques, notamment ceux pour lesquels la qualité métrique est très importante, comme l'étalonnage de caméras.

**Mots clés** : étalonnage de caméras, opérateurs d'intérêt, extraction de points avec précision subpixellaire, opérateur de Förstner, paramètres d'orientation interne.

***Abstract***

*The aim of this work is to evaluate the influence of point measurements in images, with subpixel accuracy, and its contribution in the calibration of digital cameras. Also, the effect of subpixel measurements in 3D coordinates of check points in the object space will be evaluated. With this purpose, an algorithm that allows subpixel accuracy was implemented for semi-automatic determination of points of interest, based on Förstner operator. Experiments were accomplished with a block of images acquired with the multispectral camera DuncanTech MS3100-CIR. The influence of subpixel measurements in the adjustment by Least Square Method (LSM) was evaluated by the comparison of estimated standard deviation of parameters in both situations, with manual measurement (pixel accuracy) and with subpixel estimation. Additionally, the influence of subpixel measurements in the 3D reconstruction was also analyzed. Based on the obtained results, i. e., on the quantification of the standard deviation reduction in the Inner Orientation Parameters (IOP) and also in the relative error of the 3D reconstruction, it was shown that measurements with subpixel accuracy are relevant for some tasks in Photogrammetry, mainly for those in which the metric quality is of great relevance, as Camera Calibration.*

***Keywords** : camera calibration, interest operators, extraction of points with subpixel accuracy, Förstner operator, Inner Orientation Parameters.*

***Resumo***

*O objetivo deste trabalho é avaliar a influência das medidas de pontos com qualidade subpixel, em imagens digitais, e sua contribuição na calibração de câmaras digitais. Adicionalmente, o efeito das medidas subpixel na determinação das coordenadas 3D no espaço objeto, com base em pontos de verificação, será avaliado. Visando estes objetivos e com base no operador de Förstner, um algoritmo que permite a medição de pontos com precisão subpixel e de modo semi-automático foi implementado. Experimentos foram realizados com um bloco de imagens adquiridas com a câmara multiespectral DuncanTech MS3100-CIR. A influência das medições subpixel no ajustamento pelo método dos mínimos quadrados (MMQ) foi avaliada pela comparação do desvio padrão estimado para os parâmetros em ambas as situações, com medição manual (precisão pixel) e com estimativa de qualidade subpixel. Além disso, a influência das medições subpixel na reconstrução 3D também foi analisada. Com base nos resultados obtidos, i. e., na avaliação da redução do desvio padrão nos parâmetros de orientação interior (IOP) e também no erro relativo da reconstrução 3D, foi mostrado que as medições com precisão subpixel são relevantes para algumas tarefas em Fotogrametria, principalmente para aquelas em que a qualidade métrica é de grande relevância, como calibração da câmaras.*

***Palavras-chave** : calibração de câmaras, operadores de interesse, extração de pontos com acurácia subpixel, operador de Förstner, Parâmetros de Orientação Interior.*

## 1. Introduction and objectives

The progress in Digital Photogrammetry is fast due to different factors: the development of modern Digital Photogrammetric Workstations (DPW); the development of new digital sensors, with different resolutions, both in spectral and spatial dimensions; as well as due to algorithms for image processing and analysis. Part of the researches in Digital Photogrammetry has focused on the development of algorithms that allow the automation of some photogrammetric tasks, from planning the acquisition of the data set, up to the edition and quality control of the generated products. One important aspect that is relevant for automation in this workflow refers to correspondence methods and, related to this, is the point measurement with subpixel quality.

Since the pixel size converted to the object space scale corresponds to the ground sample element, one can argue that it is not reasonable to accomplish measurements with subpixel quality. However, some papers in the Photogrammetric literature state that, depending on the desired accuracy, measurement with subpixel quality is of crucial importance and contributes to the improvement of the solution (Clarke et al. 1993; Tang et al. 1996; Zhu et al. 2007). Considering that most of softwares for image processing and photogrammetry allow the measurement of point coordinates only with pixel accuracy, Figure 1 shows some situations in which the need for subpixel methods is evidenced.

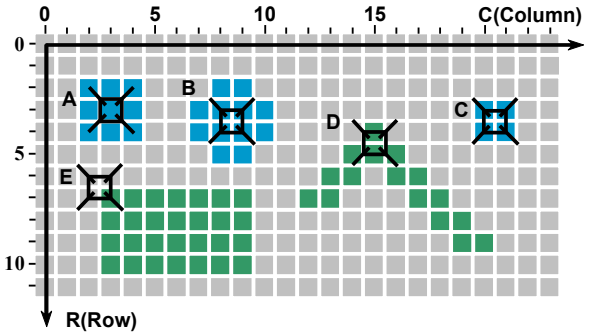


**Figure 1**: Example of five distinct points in one synthetic image.

Considering that columns and rows positions refer to each pixel center, most of the points shown in Figure 1 (as B, C, D and E) need a subpixel extraction method. Without considering subpixel method, only point A will be correctly measured as the central pixel. Considering the symmetry of the targets, the measurement with subpixel accuracy can be obtained in points B and C, based on centre of mass (centroid) approaches, in which the weighted average, using gradients or gray values as weights, for example, allows the subpixel estimation (Trinder, 1989; Otepka, 2004). Excluding points A, B and C, the remaining corner points require other techniques to properly extract the coordinates with subpixel accuracy.

There are a lot of algorithms to extract distinct points from images, with different principles, characteristics and accuracies. The comparison of methods is already well explored in the Photogrammetric and Computer Vision literature and it is out of the scope of this paper. As an example of interest operators we can mention: Moravec operator (Moravec, 1977; Tang et al. 1996; Galo et al. 2002), Förstner operator (Förstner, 1986, 1993; Förstner et al. 1987), Dreschler operator (Luhmann et al. 1986), SUSAN operator (Smith et al. 1995), Harris and Plessey operator (Harris et al. 1988; Zhu et al. 2007), SIFT (Lowe, 2004; Bay et al. 2006), SURF (Bay et al. 2006), FAST operator (Jazayeri et al. 2010) and others, as can be seen in (Giraudon et al., 1991; Wang et al., 1995; Trajkovic and Hedley, 1998; Rohr, 1997).

Tang et al. (1996) mentioned the importance of subpixel point extraction in Photogrammetry and, considering this context, the aim of this paper is to evaluate the influence of using algorithms for point extraction with subpixel accuracy in Camera Calibration process. This assessment is based on the analysis of the standard deviation of the estimated IOP and also, the influence in the 3D coordinates, in the object space. The images used in the experiments were acquired with the DuncanTech MS3100 – CIR (Color-InfraRed) camera. The subpixel point extraction algorithm implemented is specific for corner detection and is based on the Förstner operator.

## 2. Interest Operator and the subpixel method used in this work

As mentioned in the last section, there are a lot of methods to extract points of interest in digital images. In general these operators are named Interest Operators, that can be defined according to Haralick et al. (1993, p. 595) as: *"Interest Operator is a neighborhood operator that is designed to locate, with high spatial accuracy, pixel or subpixel positions whose central neighborhoods have distinctive gray tone patterns*".

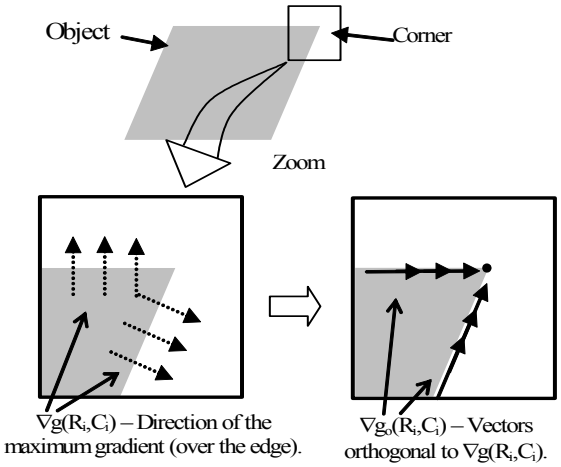


**Figure 2**: Subpixel corner estimation principle based on the intersections of vector orthogonal to the maximum gradient vectors $\nabla g(R_i,C_i)$.
Adapted from (Galo et al., 2002).

The interest points to be used in this work are corner points, since this kind of points are, in general, easy to find in images and also easy to be materialized in a test field. This kind of points can be obtained by the idea that a corner is usually located in the intersection of, at least, two edges, as can be seen in Figure 2. As can be verified in this figure, the corner can be obtained by the intersection of the edges or by the intersection of

vectors that are orthogonal to the directions of maximum gray level gradients.

Considering that the direction of maximum gradient at one pixel (Row,Column)=(R,C) is $\nabla g(R,C)$ and that the vector orthogonal to this vector is $\nabla g_o(R,C)$, the intersection of all vectors $\nabla g_o(R,C)$ in a neighborhood of one corner point allows the estimation of this corner position. Representing one generic point i on the edge by $(R_i,C_i)$, the corner position to be determined by $(R_o,C_o)$, and considering the straight line equation in polar mode, the following equation can be written:

$$n_i = \rho(R_i,C_i) - R_o\cos\theta - C_o\sin\theta = 0 \qquad (1)$$

where $n_i$ represents the distance between the point $(R_o,C_o)$ and the straight line defined by $(\rho,\theta)$, as shown in Figure 3.

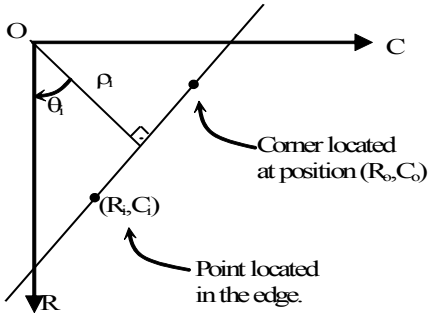


**Figure 3**: Corner position at $(R_o,C_o)$ and edge passing through point $(R_i,C_i)$.
Adapted from (Förstner et al., 1987).

Assuming that inside one window with m elements one corner point exists, with coordinates $(R_o, C_o)$, one system of equations can be written by using Equation 1, in which the parameters $R_o$ and $C_o$ can be estimated using the Least Squares Method (LSM). Considering that only points belonging to edges can contribute to corner localization, the magnitude of the gradient can be used as a weight factor, as proposed by Förstner et al. (1987) and Förstner (1993, p. 336). Under these assumptions, the following function can be written:

$$\Omega(\hat{R}_o,\hat{C}_o) = \sum_{i=1}^{m}\left(\rho(R_i,C_i) - \hat{R}_o\cos\theta_i - \hat{C}_o\sin\theta_i\right)^2 w_i \qquad (2)$$

Where $w_i = ||\nabla g_i||^2 = g_{Ri}^2 + g_{Ci}^2$ is the weight function, based on the $g_{Ri}$ and $g_{Ci}$, that are the components of the gradient along rows and columns, respectively. The corner position $(\hat{R}_o,\hat{C}_o)$ can be estimated considering that these point coordinates minimize the Functions 2 and 3.

$$\Omega(\hat{R}_o,\hat{C}_o) = \sum_{i=1}^{m}\left(\rho(R_i,C_i) - \hat{R}_o\cos\theta_i - \hat{C}_o\sin\theta_i\right)^2\left(g_{Ri}^2 + g_{Ci}^2\right) \qquad (3)$$

From Equation 3 it is possible to write the partial derivatives of this equation with respect to $\hat{R}_o$ and $\hat{C}_o$ and to write one system of equations composed by m equations and two unknowns. After that, the parameters can be grouped and it is possible to write Equation 4:

$$\begin{bmatrix}\sum\cos^2(\theta_i)w_i & \sum\sin\theta_i\cos\theta_i w_i\\ \sum\sin\theta_i\cos\theta_i w_i & \sum\sin^2(\theta_i)w_i\end{bmatrix}\begin{bmatrix}\hat{R}_o\\ \hat{C}_o\end{bmatrix} = \begin{bmatrix}\sum\rho_i\cos\theta_i w_i\\ \sum\rho_i\sin\theta_i w_i\end{bmatrix} \qquad (4)$$

that can be used to determine the unknowns by:

$$\begin{bmatrix}\hat{R}_o\\ \hat{C}_o\end{bmatrix} = \begin{bmatrix}\sum g_{Ri}^2 & \sum g_{Ri}g_{Ci}\\ \sum g_{Ci}g_{Ri} & \sum g_{Ci}^2\end{bmatrix}^{-1}\begin{bmatrix}\sum(R_i g_{Ri}^2 + C_i g_{Ri}g_{Ci})\\ \sum(C_i g_{Ci}^2 + R_i g_{Ri}g_{Ci})\end{bmatrix} \qquad (5)$$

The previous developments were based on Förstner (1993, p. 341) and Förstner et al. (1987). It is relevant to mention that the 2x2 matrix appearing in Equation 5 is exactly the matrix used by the Förstner operator, as can be observed in Förstner (1986, p. 136), Luhmann et al. (1986, p. 467) and Rohr (1997, p. 220). It is also important to mention that with some modifications, the same principle can be used to locate and classify other kinds of points of interest, as can be seen in Förstner (1993).

Different operators can be used to compute the gradients in rows and columns directions, such as Sobel masks, for example, which were used in this work. In the above description it is assumed that the approximated position of the corner point is given, and around this point one window with m pixels is defined. The definition of the approximated point coordinates can be made manually, semi-automatically or automatically. To avoid the presence of false corner points, as usually happens in the automatic approaches, in this work the approximated position was measured manually, with pixel accuracy, and the above approach was applied only to refine the corner point coordinates to subpixel accuracy.

In the implementation of the described approach to determine the subpixel position, the user can choose the size of the matrix around the corner point and, for convenience, windows with odd numbers of pixels were used.

## 3. Camera calibration model

Camera calibration can be performed by different methods and in Photogrammetry the basic model usually used is based on the well known Collinearity Equations:

$$x = -c\frac{N_x}{D}$$
$$y = -c\frac{N_y}{D} \qquad (6)$$

where:

$$\begin{aligned} N_X &= m_{11}(X-X_{cp}) + m_{12}(Y-Y_{cp}) + m_{13}(Z-Z_{cp})\\ N_Y &= m_{21}(X-X_{cp}) + m_{22}(Y-Y_{cp}) + m_{23}(Z-Z_{cp})\\ N_Z &= m_{31}(X-X_{cp}) + m_{32}(Y-Y_{cp}) + m_{33}(Z-Z_{cp}) \end{aligned} \qquad (7)$$

and c is the camera focal length; $(X_{cp},Y_{cp},Z_{cp})$ are the 3D coordinates of the perspective center in the object space; (X,Y,Z) are the coordinates in the object space of a point corresponding to an image point (x,y), $m_{ij}$ are the elements of the rotation matrix, computed as functions of the Euler angles ω, φ and κ around the axis X, Y and Z, respectively, as can be seen in (Mikhail et al., 2001).

Equation 6 is valid for an ideal situation in which the image point (x,y) is given in a coordinate system with origin in the principal point and where no distortions

exist. For this reason, the coordinates (x, y) can be related to the measured position (x', y'), the principal point coordinates ($x_0$,$y_0$) and the error model (Δx, Δy), i.e.:

$$\begin{bmatrix} x \\ y \end{bmatrix} = \begin{bmatrix} x' \\ y' \end{bmatrix} - \begin{bmatrix} x_0 \\ y_0 \end{bmatrix} - \begin{bmatrix} \Delta x \\ \Delta y \end{bmatrix} \quad (8)$$

where (Δx, Δy) represent functions that can be used to model systematic effects as radial symmetric distortion, decentring distortion and affinity distortion, for example. Considering these three components, the error model can be written as:

$$\begin{bmatrix} \Delta x \\ \Delta y \end{bmatrix} = \begin{bmatrix} \delta x_r \\ \delta y_r \end{bmatrix} + \begin{bmatrix} \delta x_d \\ \delta y_d \end{bmatrix} + \begin{bmatrix} \delta x_a \\ \delta y_a \end{bmatrix} \quad (9)$$

Usually, the radial symmetric distortion is modeled by the set of parameters ($k_1$, $k_2$, $k_3$) and the decentring distortion by the coefficients ($P_1$, $P_2$) (Brown, 1966). The affinity model can be modeled by the parameters (A, B) (Moniwa, 1972) or by other sets of parameters as ($A_1$, $A_2$), according to Habib et al. (2003, 2005); and also ($b_1$, $b_2$), called in-plane distortion, as can be seen in (Fraser, 1997; Dörstel et al., 2003). The measured position (x', y') that appears in Equation8 refers to a right hand 2D Cartesian system whose origin is at the center of the frame and x' is counted along each image line.

The experiments described in Section 5 were performed using in-house developed software (CC – Camera Calibration), which is based on collinearity equations. This software allows choosing the additional parameters to be included in the adjustment computations by LSM (Galo, 1993). The set of IOP that can be chosen are: the camera focal length (c); principal point position ($x_0$, $y_0$); radial lens distortion coefficients ($k_1$, $k_2$, $k_3$); decentring distortion coefficients ($P_1$, $P_2$) and affinity parameters (A, B).

## 4. Camera used in the experiments

The camera used in the experiments is a DuncanTech MS3100 – CIR multispectral camera (Figure 4a). This camera has three array sensors based on Charge Couple Device (CCD) technology.

Each array has dimensions of 6.4 mm(h)□4.8 mm(v) and between the lenses and each CCD sensor there are optical elements (Figure 4b) as prisms, filters and dichroic coats (Hi-Tech, 2005). The two dichroic coats split the energy in specific wavelengths and, in the case of the used camera the channels are: infra-red (IR), red (R) and green (G).

Considering that the aim of this work is to evaluate the influence of subpixel measurements, all the images used in the experiments were in Color Infra-Red mode (CIR). Although the results between channels R, G and IR can be different, as can be seen in Galo et al. (2006), the relative results obtained in this paper will not be affected by these differences, since only one channel is considered in all the experiments.

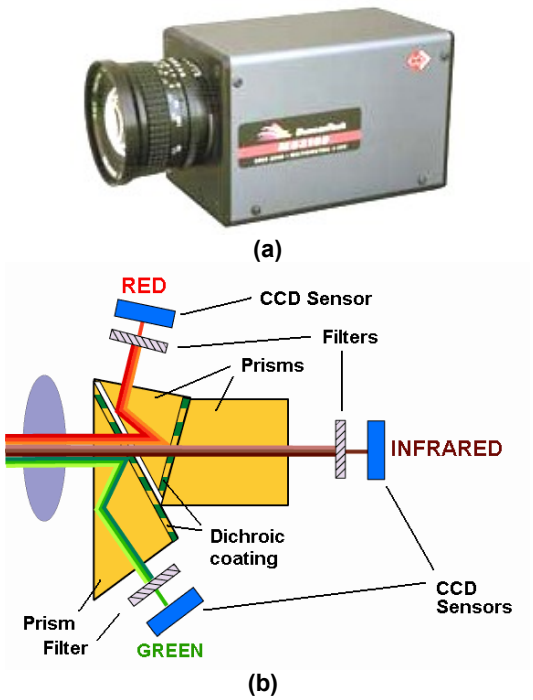


**Figure 4**: **(a)** DuncanTech MS3100 Camera, and **(b)** its internal geometry and components. Adapted from (Hi-Tech, 2005).

## 5. Experiments and discussions

In this section the experiments are described and the results discussed. Basically, three experiments were performed. The first one is related to the evaluation of the quality of the subpixel extraction technique described in section 2, applied to a synthetic image with corner points. In the second experiment the IOP, obtained in the camera calibration process, with the inputs being the coordinates measured manually and with subpixel accuracy are compared. In the third experiment the 3D coordinates in the object space are compared, when the two sets of coordinates are used.

### 5.1. Analysis of points extracted semi-automatically

In this experiment one simulated image was created, containing different synthetic targets. In this way it was possible to measure different kinds of corner points (with different numbers of edges and different angles). Since all the selected points have their positions known, these coordinates are used as a reference in the accuracy analysis. Although in this experiment the targets are synthetic, the idea is to estimate the accuracy of the extraction technique, even knowing that resolution, contrast, etc, affect the quality of real images. So, it is not expected that the same RMSE should be achieved with targets measured in real images.

In Figure 5, ten corner points are shown. For each corner two points are shown: the initial position (with symbol □, measured manually and used as an input to the algorithm) and the corner points extracted by the algorithm. The positions measured manually have pixel accuracy and since the reference coordinates are previously known, the errors were computed, as summarized in Table 1.

Observing Figure 5 it is possible to verify visually the approximated point and the estimated subpixel coordinates. Based on the quantitative analysis presented in Table 1, the average error and the RMSE for the ten points are 1/12.3 and 1/7.6 pixel, respectively. The point with the highest error (less than 0.4 pixel) is the point #8, which is a corner obtained by the intersection of three edges. Excluding this point and updating the statistics, the average error and RMSE are reduced to 1/21.0 and 1/18.9, respectively. By analyzing these results it is possible to verify the accuracy of the subpixel point extraction based on Förstner operator, that results in a RMSE of almost 1/18.9 pixel for the synthetic targets used in this experiment.

| Point Number | Detail of each Point | Point number | Detail of each point |
|---|---|---|---|
| 1 | 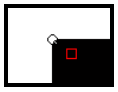 | 6 | 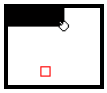 |
| 2 | 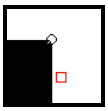 | 7 | 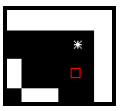 |
| 3 | 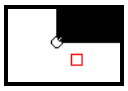 | 8 | 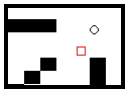 |
| 4 | 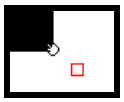 | 9 | 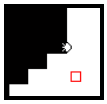 |
| 5 | 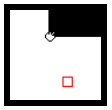 | 10 | 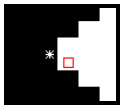 |

**Figure 5**: The set of points selected from a synthetic image used to compute the RMSE in subpixel point extraction.

| Point | $C_r$, $R_r$ (pixel) | $C_{sp}$, $R_{sp}$ (pixel) | $\Delta C$, $\Delta R$ (pixel) | Res. (pixel) |
|---|---|---|---|---|
| 1 | 22.5, 39.5 | 22.520, 39.520 | 0.020, 0.020 | 0.029 |
| 2 | 52.5, 39.5 | 52.485, 39.525 | -0.015, 0.025 | 0.029 |
| 3 | 22.5, 73.5 | 22.525, 73.480 | 0.025, -0.020 | 0.032 |
| 4 | 52.5, 73.5 | 52.476, 73.476 | -0.024, -0.024 | 0.034 |
| 5 | 93.5, 91.5 | 93.532, 91.481 | 0.032, -0.019 | 0.037 |
| 6 | 114.5, 91.5 | 114.468, 91.481 | -0.032, -0.019 | 0.037 |
| 7 | 221.0, 31.0 | 221.061, 30.988 | 0.061, -0.012 | 0.062 |
| 8 | 223.0, 80.0 | 222.779, 80.315 | -0.221, 0.315 | 0.385 |
| 9 | 209.5, 151.0 | 209.487, 151.066 | -0.013, 0.066 | 0.067 |
| 10 | 178.0, 182.5 | 178.099, 182.518 | 0.099, 0.018 | 0.100 |
| | | *Average (pixels)* | -0.007, 0.035 | **1/12.3** |
| | | *RMSE (pixels)* | 0.081, 0.103 | **1/7.6** |
| The same statistics without considering point 8 above | | | | |
| | | *Average (pixels)* | 0.017, 0.004 | **1/21.0** |
| | | *RMSE (pixels)* | 0.044, 0.029 | **1/18.9** |

($C_r$, $R_r$) – Reference coordinates (Column, Row)
($C_{sp}$, $R_{sp}$) – Subpixel coordinates
($\Delta C$, $\Delta R$)=($C_{sp}$-$C_r$, $R_{sp}$-$R_r$) - Errors in columns and rows
Res – Resultant error in each point: $Res = \sqrt{\Delta C^2 + \Delta R^2}$

**Table 1**: Accuracy in the semi-automatic point extraction algorithm.

### 5.2. The influence of subpixel extraction in camera calibration

As mentioned in the previous sections, camera calibration trials were performed using an in-house developed software. Since different sets of IOP can be used and the aim of this paper is to compare the effect of subpixel extraction in the calibration process, only one set of IOP was considered: c, $x_0$, $y_0$, and $k_1$. This set of IOP was chosen for this camera, considering that they result in the lower variance for the focal length, between seven different sets of parameters, as shown in (Galo et al., 2006).

One test field was established based on points and lines (not used in this work). These entities were marked in one wall with the help of one metallic rule and one invar plate. For the calibration purpose, ten images were acquired in CIR mode, which are shown in Figure 6.

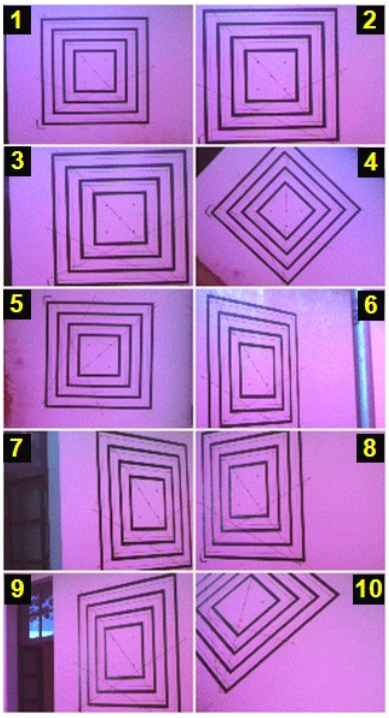


**Figure 6**: Images used in the calibration.

As can be observed, the images were collected considering different scales and rotation angles (ω, φ, κ), to reduce the correlations between some IOP and Exterior Orientation Parameters (EOP). All the points in

those ten images were measured manually (pixel accuracy) and these points were used as initial positions in the subpixel corner estimation algorithm. In Figure 7 it is possible to see the distribution of all points measured (326 in total). This distribution is important to verify if there are points in all parts of the image plane.

In Table 2 the IOP computed from the calibrations are shown in three situations: when points were measured manually (second column) and when subpixel refinement was used (third and fourth columns). Since in the subpixel approach it is necessary to define one window around the initial points, two sizes of windows were analyzed: m=9x9 and m=15x15 (See Equation 3).

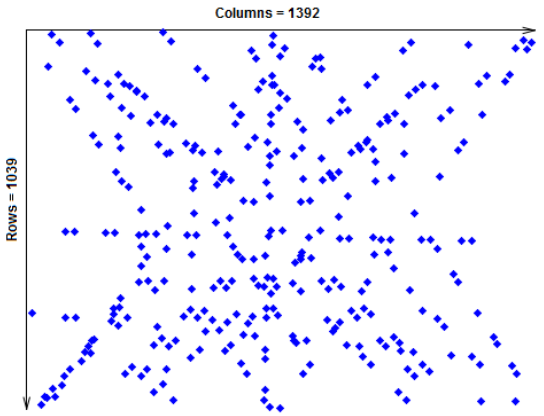


**Figure 7**: Distribution of all points measured in image plane, considering all images.

| IOP | Image CIR [Pixel] | Image CIR [subpixel] m=9x9 | Image CIR [subpixel] m=15x15 |
|---|---|---|---|
| **c** (mm) | 16.5514<br>± 0.0411<br>8.74 [pixel] | 16.5420<br>± 0.0291<br>6.20 [pixel] | 16.5737<br>± 0.0275<br>5.84 [pixel] |
| $\mathbf{x_0}$ (mm) | -0.0124<br>± 0.0305 | -0.0592<br>± 0.0224 | -0.0532<br>± 0.0208 |
| $\mathbf{y_0}$ (mm) | -0.1804<br>± 0.0426 | -0.0164<br>± 0.0292 | -0.0561<br>± 0.0282 |
| $\mathbf{k_1}$ ($mm^{-1}$) | -0.0003874<br>± 0.0000272 | -0.0003450<br>± 0.0000194 | -0.0003727<br>± 0.0000182 |

**Table 2**: IOP and respective estimated standard deviation from the adjustment by LSM for measurements with pixel and subpixel quality.

As can be seen in Table 2, the standard deviations of all estimated IOP were reduced when the subpixel measurement technique was used, compared with the observations performed manually. Based on the ratio between $\sigma_{SP}$ and $\sigma_P$, the reduction factor (RF) for each estimated IOP was computed (see Table 3).

In this table, the value of the reduction factor for the focal length ($RF_\sigma$) was computed by $RF_\sigma(c)$= 0.0291/0.0411~0.71. In average, the $RF_\sigma$ for all the IOP set is 0.67, when windows with 15x15 pixels were used in the subpixel corner estimation. By analyzing Tables 2 and 3 it is possible to verify that when subpixel estimation coordinates were used, the standard deviation of the IOP was reduced by a factor around 0.70.

| IOP | $RF_\sigma$ (m = 9x9) | $RF_\sigma$ (m = 15x15) |
|---|---|---|
| **c** (mm) | 0.71 | 0.67 |
| $\mathbf{x_0}$ (mm) | 0.73 | 0.68 |
| $\mathbf{y_0}$ (mm) | 0.69 | 0.66 |
| $\mathbf{k_1}$ ($mm^{-1}$) | 0.71 | 0.67 |
| *Average* | *0.71* | *0.67* |

**Table 3**: The values of the reduction factor in σ for each IOP.

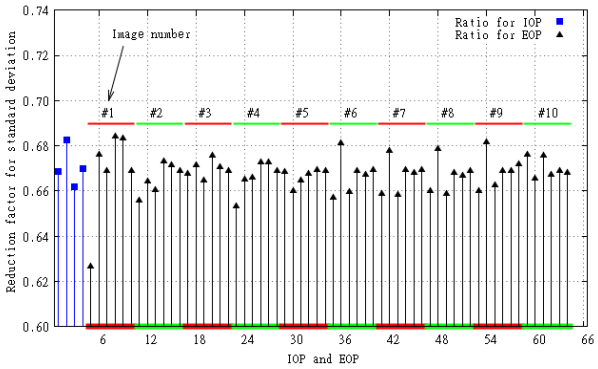


**Figure 8**: The reduction factor for all IOP and EOP, computed as the ratio $\sigma_{SP}/\sigma_P$.

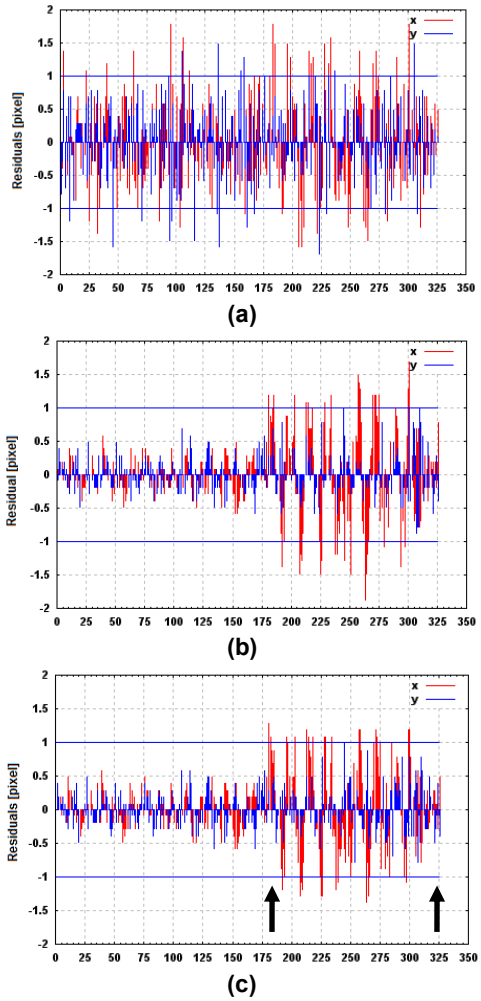


**(a)**

**(b)**

**(c)**

**Figure 9**: The residuals in x and y coordinates (in image space and in pixels units) after the calibration: **(a)** with points measured manually; **(b)** with points measured with subpixel and window size with 9x9 pixels; and **(c)** with window with 15x15 pixels.

In Tables 2 and 3 only the IOP were considered. In Figure 8 the reduction factors are shown both for the IOP and the EOP, for the case in which m=15x15.
As can be observed in this figure, the reduction factors obtained for the EOP are similar to those shown in Table 3 (column 3) for the IOP. Besides the reduction factor obtained, it is also possible to see the contribution of the subpixel estimations in the calibration process by the analysis of the residuals in image space as shown in Figure 9.

By comparing the residuals in Figure 9a with those in b and c, it is clearly visible the reduction in the residuals. Also, it is noticeable that not all residuals were reduced in the same extent. Those that are between the arrows (in Figure 9c) were less affected and these residuals correspond to the observations in images 6 to 10 (see Figure 6). Considering these results, it is possible to note that, despite the reductions in the residuals when subpixel coordinates are used, the reduction is lower for the images with high convergence, indicating that, although this geometry is very important to mitigate the effects of correlation between some IOP and EOP in the calibration process, some improvements in the feature extraction are still necessary.

### 5.3. The influence of subpixel extraction on 3D reconstruction

In the previous section, three sets of IOP were obtained (see Table 2). In this experiment two of these groups of parameters were used to compute the 3D coordinates from a set of three images. One set of IOP was estimated from coordinates measured with pixel accuracy whilst the other one corresponds to the IOPs with lower standard deviation (subpixel measurements and m=15x15). The 3D reconstruction was made using the same software used in the calibration step, but in double bundle triangulation mode, that was achieved by applying constraints in the IOP. In this processing the number of control points was 5 and the others (23) were used as check points. The accuracy of the 3D reconstruction was then estimated.

The images used in this experiment were the images 6, 1 and 9 (Figure 6), the relative positions of which in the test field are shown in Figure 10 (CP1, CP2 and CP3 are camera positions). These images were chosen based on the high base/height ratio (around 2.1 for the pair CP2 – CP3). In Figure 11 the distribution of the ground control points and the check points used in this experiment is shown.

A fter the 3D reconstruction, the errors in all 3D coordinates were computed. The experiment in which pixel accuracy measurements were used, achieved errors in depth (altimetry) of $RMSE_Z$=2.731 mm and in planimetry (XY) $RMSE_{XY}$=2.093 mm in the object space. Since the errors in the object space are related to the distance between camera–targets, the ratio between the RMSE and the average distance between the cameras and the 23 check points were estimated. The relative errors were computed for both planimetry and altimetry by $RMSE_{XY}/\overline{D}$ and $RMSE_Z/\overline{D}$, respectively. Besides these relative errors, the reduction factors in planimetry and altimetry were also computed, as shown in Table 4.

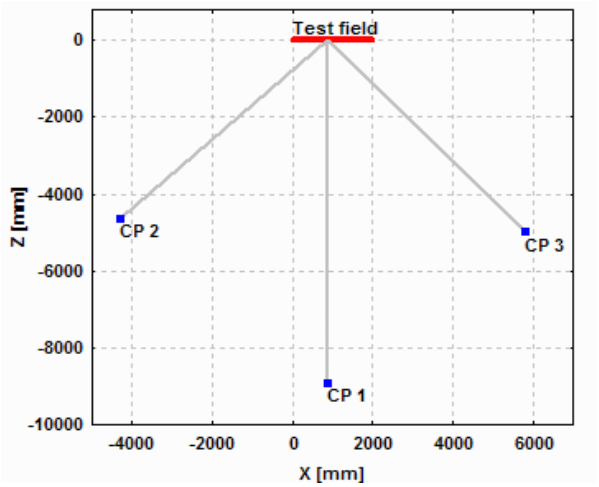


**Figure 10**: Camera positions related to the test field for the third experiment.

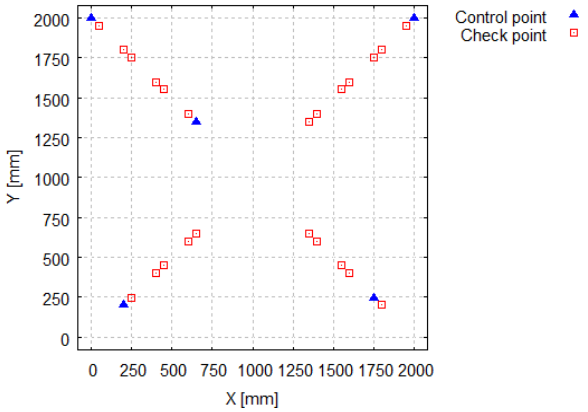


**Figure 11**: Ground control points and check points used in the 3D reconstruction analysis.

| Relative Error | $RMSE_{XY}/\overline{D}$ c $x_0$ $y_0$ $k_1$ | $RMSE_Z/\overline{D}$ c $x_0$ $y_0$ $k_1$ |
|---|---|---|
| **Image in CIR mode (P)** | 1/2952 | 1/2262 |
| **Image in CIR mode (SP)** | 1/4753 | 1/2657 |
| **Reduction factor in relative error** | 0.62 | 0.82 |

**Table 4**: Relative error in planimetry and altimetry and the reduction factor in relative error when pixel (P) and subpixel (SP) quality were considered.

From these results it is possible to observe the errors reduction in 3D reconstruction when subpixel measurements are used. It is also possible to verify that the measurements with subpixel accuracy had more influence in planimetry than in altimetry, since the reduction factor in planimetry is lower than the reduction factor in altimetry.

## 6. Conclusions

The main purpose of this work was to verify the influence of measuring points with subpixel accuracy in the calibration of one digital camera and also the effects of these measurements in 3D reconstruction. To perform the analysis one interest operator based on Förstner approach was implemented and it was

considered that the coordinates of an initial corner point was given as an input to the algorithm, so, the algorithm runs in a semi-automatic mode. The images used in the experiments were images in a color infra-red (CIR) mode, acquired by the DuncanTech MS3100 multispectral camera.

The evaluation of the subpixel extraction technique was performed considering some simulated targets, with known corner positions. The results of the experiments indicated that the average errors can achieve 1/21 pixel and a RMSE of 1/18.9 pixel. Although the quality of subpixel extraction is evident, the magnitude of these errors corresponds to the synthetic targets used in this work and can not be generalized for corners in real images.
Assuming that $\sigma_{IOP(i)}$ is the standard deviation of one IOP(i), estimated by a set of points with pixel level accuracy, the standard deviations of the estimated IOP(i) when subpixel measurements are used is reduced to $0.7x\sigma_{IOP(i)}$. This result indicates the reduction in the dispersion of IOP when subpixel measurements are used.

The evaluation of the results in 3D reconstruction indicates that in planimetry the reduction factor in the relative error was around 0.62. In altimetry this factor was 0.82. Although the subpixel measurements reduced the error in both planimetry and altimetry, the effects in planimetry were more effective. This can be partially explained by the type of algorithm, in which the points were measured independently in each image, with no comparison between images, as in the Least Squares Matching technique.

All the experiments performed and discussed indicated that the use of subpixel point extraction techniques improves the quality of the IOP estimated during the camera calibration process and also the 3D coordinates estimated in the Photogrammetric process. These results indicate that mainly for those applications in which high positional accuracy is necessary, the subpixel estimation improves the results.

It is important to highlight that camera calibration and 3D reconstruction from images are function of different factors as: the camera used, the quality of the observations, algorithms and geometry of the acquisition. Therefore, it is straightforward to consider that for different systems, the general behavior achieved in this work will be similar, but the reduction factors can not be generalized for others systems.

## Acknowledgments

The authors express their acknowledgements to the following people and institutions:

- CNPq - Conselho Nacional de Desenvolvimento Científico e Tecnológico by the support in the followings projects: 475932/2003-0; 481047/2004-2; 478782/2009-8; and 312909/2009-8.
- FAPESP - Fundação de Amparo à Pesquisa do Estado de São Paulo (Project 1997/10956-0).
- To the Cart. Engineers Sandra Stephan de Souza Telles and Annette Pic for the materialization of the test field used in the experiments.

## References

Bay, H., Tuytelaars, T., Van Gool, L., 2006. SURF: Speeded Up Robust Features. In: Proc. European Conference on Computer Vision, pp. 404-417, Graz, Austria.

Brown, D.C., 1966. Decentering distortion of lenses. Photogrammetric Engineering 32(3), 444-462.

Clarke, T.A., Cooper, M.A.R., Fryer, J.G., 1993. An estimator for the random error in subpixel target location and its use in the bundle adjustment. In: Optical 3D measurements techniques, pp. 161-168, Zürich, Switzerland.

Dörstel, C., Jacobsen, K., Stallmann, D., 2003. DMC – Photogrammetric Accuracy – Calibration Aspects and Generation of Synthetic DMC Images. In: Optical 3D measurements techniques, pp. 74-82, Zürich, Switzerland.

Förstner, W., 1986. A feature based correspondence algorithm for image matching. International Archives of Photogrammetry and Remote Sensing XXVI (Part 3/3), 150-166.

Förstner, W., 1993. Image matching. In: Haralick, R. M; Shapiro, L.G. Computer and Robot Vision, Chap. 16, Vol. II, pp. 289-379. Reading: Addison-Wesley Publishing Company.

Förstner, W., Gülch, E., 1987. A fast operator for detection and precise location of distinct points, corners and centres of circular features. In: ISPRS Intercommission Workshop, Interlaken, Switzerland.

Fraser, C.S., 1997. Digital camera self-calibration. ISPRS Journal of Photogrammetry and Remote Sensing 52(4), 149-159.

Galo, M., 1993. Calibração e aplicação de câmaras digitais. Dissertação de Mestrado, Curso de Pós-Graduação em Ciências Geodésicas, Universidade Federal do Paraná, Curitiba - PR, Brazil, 151p.

Galo, M., Tozzi, C.L., 2002. Extração de pontos com acurácia subpixel em imagens digitais. In: MITISHITA. Edson Aparecido. (Org.). Série em Ciências Geodésicas - Pesquisa em Ciências Geodésicas - 2002. Curitiba. v. 2. pp. 289-313. ISBN: 85-88783-03-7.

Galo, M., Hasegawa, J.K., Tommaselli, A.M.G., Imai, N.N., 2006. Registration analysis and inner calibration of a three CCD multispectral frame camera. In: EUROCOW 2006 - International Calibration and Orientation Workshop, Castelldefels, Spain.

Giraudon, G., Deriche, R., 1991. On corner and vertex detection. INRIA - Institut National de Recherche en Informatique et en Automatique. Technical Report 1439, 35p.

Habib, A., Morgan, M., 2003. Small format digital cameras for mapping applications: calibration and stability analysis. In: Mitishita, Edson Aparecido. (Org.). Série em Ciências Geodésicas – Novos Desenvolvimentos em Ciências Geodésicas - 2003. Curitiba, v. 3, p. 3-25. ISBN: 85-88783-04-05.

Habib, A., Morgan, M., 2005. Stability analysis and geometric calibration of off-the-shelf digital cameras. Photogrammetric Engineering & Remote Sensing 71(6), 733-741.

Haralick. R.M., Shapiro. L.G., 1993. Computer and robot vision - Vol. II. Reading: Addison-Wesley Publishing Company, 630 p.

Harris, C., Stephens, M., 1988. A Combined corner and edge detector. In: Proc. Fourth Alvey Vision Conference, Manchester, UK, pp. 147-151.

Hi-Tech Electronics, 2005. Spectral Configuration Guide for DuncanTech 3-CCD Cameras. http://www.hitech.com.sg. (Accessed 01 Feb. 2005)

Jazayeri, I., Fraser C.S., 2010. Interest operators for feature-based matching in Close Range Photogrammetry. Photogrammetric Record 25(129), 24-41.

Lowe, D.G., 2004. Distinctive image features from scale-invariant keypoints. International Journal of Computer Vision 60(2), 91-110.

Luhmann, T., Altrogge. G., 1986. Interest-operator for image matching. International Archives of Photogrammetry and Remote Sensing XXVI(3/2), 459-474.

Mikhail, E.M., Bethel, J., Mcglone, J.C., 2001. Introduction to Modern Photogrammetry. John Wiley & Sons, Inc.: New York City, NY, USA, 479p.

Moravec. H.P., 1977. Towards automatic visual obstacle avoidance. In: Proc. of the 5th Int. Joint Conference on Artificial Intelligence. Cambridge, UK.

Otepka, J.O., 2004. Precision target mensuration in vision metrology. PhD Thesis, University of Technology Vienna, Austria, 86p.

Redlake Masd, 2003. MegaPlus® MS3100 Multi-Spectral Camera. http://www.redlake.com (Accessed 06 Dec. 2004)

Rohr. K., 1997. On 3D differential operators for detecting point landmarks. Image and Vision Computing 15(3), 219-233.

Smith. S.M., Brady, J.M., 1995. SUSAN - A New Approach to Low Level Image Processing. DRA - Defense Research Agency Technical Report TR95SMS1c. Hampshire, UK. 59p.

Tang. L., Heipke. C., 1996. Automatic Relative Orientation of Aerial Images. Photogrammetric Engineering & Remote Sensing 62(1), 47-55.

Trajkovic, M., Hedley, M., 1998. Fast Corner detection. Image and Vision Computing 16(2), 75-87.

Trinder, J.C., 1989. Precision of digital target location. Photogrammetric Engineering & Remote Sensing 55(6), 883-886.

Zhu, Q., Wu, B., Wan, N., 2007. A sub-pixel location method for interest points by means of the HARRIS interest strength. Photogrammetric Record 22(120), 321-335.

Wang, H., Brady, M., 1995. Real-time corner detection algorithm for motion estimation. Image and Vision Computing 13(9), 695-703.